Article

Evidence for large thermodynamic signatures of in-gap fermionic quasiparticle states in a Kondo insulator

Zhuo Yang [1], Christophe Marcenat [2] ✉, Sunghoon Kim [3], Shusaku Imajo [1], Motoi Kimata[4], Toshihiro Nomura [1,5], Albin Muer[6], Duncan K. Maude[6], Fumitoshi Iga [7,8], Thierry Klein[9], Debanjan Chowdhury [3] ✉ & Yoshimitsu Kohama [1] ✉

The mixed-valence compound YbB_{12} displays paradoxical quantum oscillations in electrical resistivity and magnetic torque in a regime with a well-developed insulating charge gap and in the absence of an electronic Fermi surface. However, signatures of such unusual fermionic quasiparticles in other bulk thermodynamic observables have been missing. Here we report the observation of a series of sharp double-peak features in the specific heat as a function of the magnetic field. The measured Hall resistivity evolves smoothly across the field values at which the characteristic anomalies appear in the thermodynamic response and rules out the possibility of conventional electrons as their origin. Our observations of thermodynamic anomalies in a bulk three-dimensional electrical insulator provide the evidence for the presence of emergent dispersing fermionic excitations within the insulating bulk, which sets the stage for further investigation of electron fractionalization in other correlated mixed-valence compounds.

Quantum oscillations are widely used to map out the Fermi surfaces in metals and can be understood in the semi-classical limit as arising from the cyclotron motion of electrons. However, the observation of quantum oscillations in electrical insulators, such as the three-dimensional mixed-valence compounds SmB_6 and YbB_{12}[1–3], as well as certain two-dimensional semiconductors[4,5], which do not host electronic Fermi surfaces have led to a critical examination for alternative mechanisms leading to the same phenomenon[6–16]. Of particular interest are the observations in YbB_{12}, where thermal conductivity measurements at low temperatures reveal highly mobile excitations that carry heat like in a metal but do not conduct electricity[17]. The

celebrated Wiedemann-Franz law which relates the thermal and electrical conductivities in all metals at asymptotically low temperatures is violated in this material by at least three orders of magnitude[17]. However, the thermal Hall conductivity up to a field of 12 T remains negligibly small[17]. This leads to the fundamental question of whether electrically neutral excitations in an insulator, which nominally do not have a direct orbital coupling to an external magnetic field, can nevertheless display singular thermodynamic signatures characteristic of metals. Finding compelling signatures of the interaction-induced electron fractionalization and the emergence of neutral fermionic excitations, especially in the bulk thermodynamic response, remains

[1]Institute for Solid State Physics, The University of Tokyo, Kashiwa, Chiba 277-8581, Japan. [2]Univ. Grenoble Alpes, CEA, Grenoble INP, IRIG, Pheliqs, 38000 Grenoble, France. [3]Department of Physics, Cornell University, Ithaca, NY 14853, USA. [4]Institute for Materials Research, Tohoku University, Sendai, Miyagi 980-8577, Japan. [5]Department of Physics, Faculty of Science, Shizuoka University, Shizuoka 422-8529, Japan. [6]Laboratoire National des Champs Magnétiques Intenses (LNCMI-EMFL), CNRS, UGA, UPS, INSA, 38042 Grenoble/Toulouse, France. [7]Institute of Quantum Beam Science, Graduate School of Science and Engineering, Ibaraki University, Mito 310-8512, Japan. [8]Research and Education Center for Atomic Sciences, Ibaraki University, Tokai, Ibaraki 319-1106, Japan. [9]Univ. Grenoble Alpes, CNRS, Institut Néel, 38000 Grenoble, France. ✉e-mail: christophe.marcenat@neel.cnrs.fr; debanjanchowdhury@cornell.edu; ykohama@issp.u-tokyo.ac.jp

one of the outstanding challenges in the study of correlated quantum materials, including mixed-valence compounds.

Quantum oscillations in high-quality single crystals of YbB_{12} have been reported in both magnetoresistance and magnetic torque, with large sinusoidal oscillations periodic in $1/B$ above 38 T[2,17,18]. Moreover, the functional form of the oscillatory components is well described by Lifshitz–Kosevich (LK) theory[19,20], suggesting a fermionic origin tied to the underlying Fermi-Dirac distribution function. However, this material has an appreciable negative magnetoresistance, and the charge-gap decreases with increasing magnetic field[18,21,22], ultimately resulting in a field-induced insulator-metal transition around $B = 46$ T[21,23,24]. Relatedly, the Hall resistance exhibits clear anomalies in the quantum oscillation regime[18], making it difficult to disentangle the effects of electronic charge carriers from the possibly neutral carriers on the oscillation phenomenology. As a result, the microscopic origin of the low-energy excitations that are responsible for both the oscillations and the metallic-like thermal conductivity of YbB_{12} in the insulating regime remains unclear[17,18]. To shed new light on these pressing questions, we present here a detailed study of thermodynamic properties of YbB_{12} in a magnetic field, which provides evidence for bulk sub-gap excitations with a fermionic character that are distinct from electrons.

Results

We report here a sequence of increasingly pronounced (singular) features in both the specific heat (C) and the magnetocaloric effect (MCE) within the insulating phase of YbB_{12}. These features, characterized by a series of "double-peak" features in the specific heat at 11, 16, 19.6, and 30 T, respectively, suggest an underlying fermionic density of states (DoS). The Hall resistivity measurement evolves smoothly across these field values, ruling out an electronic origin for these anomalies and suggesting a distinct fermionic contribution to the singular DoS in YbB_{12}. Moreover, the fourfold rotational symmetry tied

to the angle-dependent field position of the double-peak structure suggests a bulk rather than surface-state origin.

Unlike magnetoresistance, MCE and specific heat (C) are bulk-sensitive probes for the fermionic DoS. MCE represents the field dependence of the sample temperature, $T(B)$, which is a measure of the inverse of magnetic entropy S. In Fig. 1, we plot the magnetoresistance, Hall resistivity, MCE, and C/T taken at 0.65–0.7 K in fields up to 35 T. These experiments were performed on the same YbB_{12} single crystal (sample#1) with **B** along [1 0 0]. The vertical lines in Fig. 1(a)-(c) indicate the field positions of the thermodynamic anomalies. All the features shown in Fig. 1 were observed in other samples (sample#2 and sample#3, Supplementary Notes 6 and 7). As noted previously in magnetic torque and magnetoresistance measurements[2], our ρ_{xx} experiments resolve a weak feature at 19.6 and 30 T, respectively, while the thermodynamic probes (MCE and C/T) detect additional anomalies at 11, 16 T. Intriguingly, the Hall resistivity (ρ_{xy}) only exhibits an anomaly at 30 T (Supplementary Note 4). It is worth noting that while the magnetoresistance and Hall resistivity are directly sensitive to the electronic carriers at the surface and in bulk, the specific heat and MCE are bulk-sensitive probes that help detect contributions from *all* low-energy degrees of freedom.

The observation of quantum oscillations in an insulator has raised questions about the role of inhomogeneities and sample quality[1,2,25,26]. However, the observation of a residual metallic-like thermal conductivity in an electrical insulator at low temperatures presents a challenge to a simplified picture of disconnected metallic inclusions below the percolation threshold in the three-dimensional bulk of the sample. Nevertheless, to ensure that the high-quality single crystals used in this study represent the universal and intrinsic properties of YbB_{12}, we have performed additional X-ray diffraction, magnetoresistance, and MCE measurements (Supplementary Note 1 and 3). The extracted gap sizes and quantum oscillation frequencies are consistent with earlier reports[2,22,27].
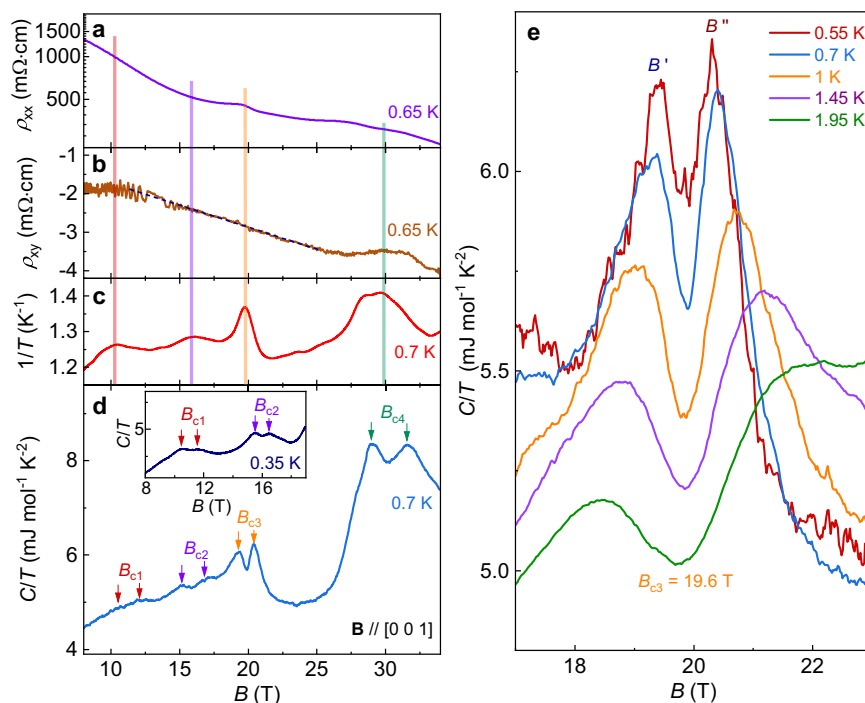

Fig. 1 | Comparison of magnetoresistance, Hall resistivity, MCE and specific heat of YbB_{12} as a function of magnetic field. a Magnetoresistance and **b** Hall resistivity of YbB_{12} as a function of the magnetic field measured at $T = 0.65$ K (see Supplementary Note 2 for a full set of transport data). **c** Reciprocal temperature (1/T) of YbB_{12} as a function of the applied magnetic field in an adiabatic condition measured at initial temperature $T = 0.7$ K. **d** Specific heat divided by temperature

C/T in YbB_{12} as a function of the magnetic field at $T = 0.7$ K. In addition to the pronounced anomalies at 16, 19.6, and 30 T, our specific heat and MCE data also resolve small anomalies at 11 T (see inset and Supplementary Note 7). **e** Specific heat C/T as a function of the magnetic field at indicated temperature, obtained by subtracting the Schottky and phonon contributions from as-measured C/T.
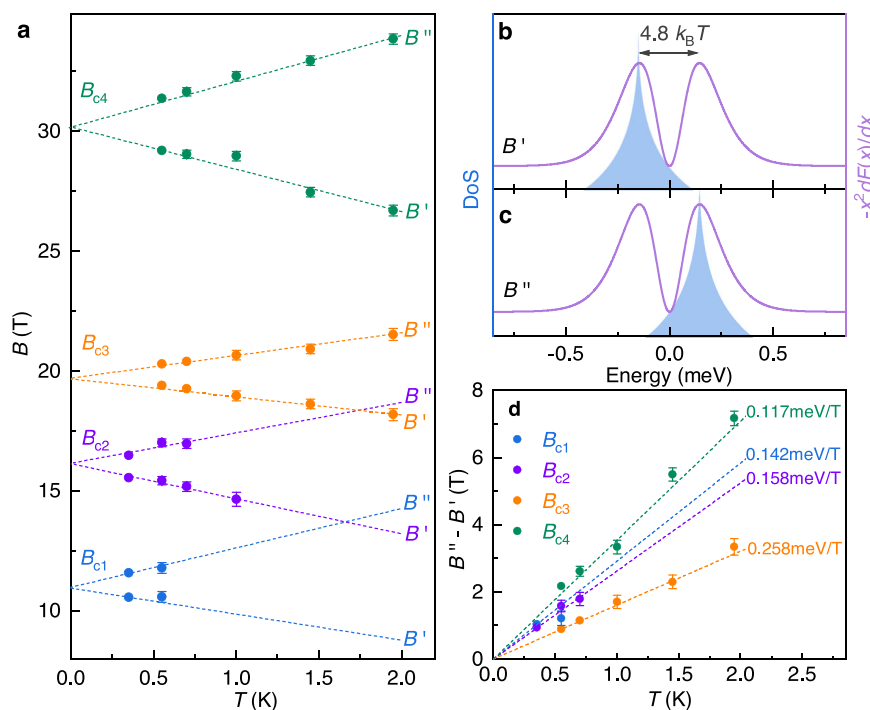
Fig. 2 | Fermionic quasiparticle−origin of the double-peak structure in C/T.
a Measured magnetic field positions of the double peaks B' and B'' as a function of temperature for all the anomalies in C/T. **b, c** Schematic view to show the origin of the double-peak structure in C/T. **d** Measured splitting ($B'' − B'$) for all the double-peak structures in C/T as a function of temperature. Dashed lines indicate the linear fit to obtain $d\epsilon/dB$ from the inverse slope. The error bars represent one standard deviation of uncertainty.

To track the evolution of the magnetic entropy of YbB$_{12}$, we plot $1/T(B)$ versus B in Fig. 1c, which exhibits well-defined local peaks with an amplitude much larger than that of the quantum oscillation (Supplementary Fig. 2b). This indicates the existence of high entropy states in the corresponding field regions. These local peaks were also observed in MCE data for different YbB$_{12}$ single crystals (sample#2; Supplementary Note 6), reflecting the reproducibility of the phenomena. The specific heat anomalies, which appear as a double-peak structure, are marked by the colored double arrows in Fig. 1d. Among them, the double-peak structures at 19.6 and 30 T are particularly pronounced, whereas the structures at 11 and 16 T are less apparent but are clearly resolved in lower temperature data (inset of Fig. 1d, Supplementary Notes 6 and 7). The simultaneous observation of single- and double-peak structures in MCE and C/T is a characteristic feature for a singularity in the DoS passing through the Fermi level, as demonstrated, e.g., in the quantum oscillation of graphite[28]. The fields B_{c1}–B_{c4} in Fig. 1d are defined as the location when a local maximum in the DoS crosses the Fermi level, corresponding to the peak positions in MCE and center positions of the double peaks in C/T. However, the key difference with graphite is that YbB$_{12}$ does not show any drastic change in ρ_{xy} across these field values[18,29]. This strongly supports the contention that the sequential anomaly in MCE and C/T is due to bulk low-energy fermionic quasiparticles that are distinct from electrons in YbB$_{12}$.

The appearance of the anomaly in C/T and MCE indicates that the signals at 11, 16, and 19.6 T are caused by the bulk states, while the absence of the anomaly in ρ_{xy} excludes its origin from the electronic transition of conventional electrons and suggests the existence of neutral fermionic quasiparticles in the bulk states. Although the field sweep of ρ_{xx} exhibits some hysteretic non-monotonic features at 16 and 19.6 T[2,18], we note that this is a non-equilibrium phenomenon amplified with faster sweep rates (Supplementary Note 5). On the other hand, the anomaly at 30 T might arise in part due to a conventional electronic transition[2,18].

Given the highly unconventional character of the bulk magnetic field dependence on the thermodynamic response of YbB$_{12}$, it is useful to compare these measurements against similar observations in more conventional materials. As demonstrated in graphite[28], the double-peak structure in C/T provides direct information on the singularities associated with the Landau levels in a magnetic field. The origin of this behavior is intimately tied to the Fermi−Dirac distribution function. When an electronic quasiparticle state contributes to the magnetic field-tuned DoS near the Fermi energy, the specific heat can be calculated as[30],

$$C/T = k_B^2 \int_{-\infty}^{\infty} D(\epsilon,B)\left(-x^2 \frac{dF(x)}{dx}\right) dx. \qquad (1)$$

Here the energies are measured relative to the Fermi energy, $x = \epsilon/k_B T$ is the ratio of energy and the thermal energy, $F(x) = 1/(1+e^x)$ is the Fermi-Dirac distribution function, and $D(\epsilon,B)$ is the DoS for the fermionic quasiparticle singularity. Specifically, the kernel function $(-x^2 d(F(x))/dx)$ exhibits two local maxima with an energy separation that increases linearly with temperature as $4.8 k_B T$[28] (Fig. 2b). In Fig. 1e, we focus on the double-peak structure in C/T at 19.6 T measured at indicated temperatures after subtracting the electron, phonon, and Schottky contributions, respectively (Supplementary Note 8). The field positions associated with the double peaks are strongly temperature dependent, and likely merge into a single peak with decreasing temperature. This feature was also observed in three additional double-peak structures (Supplementary Note 6).

We plot the position of the double-peak structures versus temperature in Fig. 2a. The splitting of the double peak decreases linearly with decreasing temperature. The central field of the double peaks remains constant and coincides with the entropy maximum observed in MCE. The measured C/T has a high sensitivity to the DoS over a finite energy interval, set by the thermal energy, near the Fermi energy. The overlap of the DoS and the kernel function features two local maxima
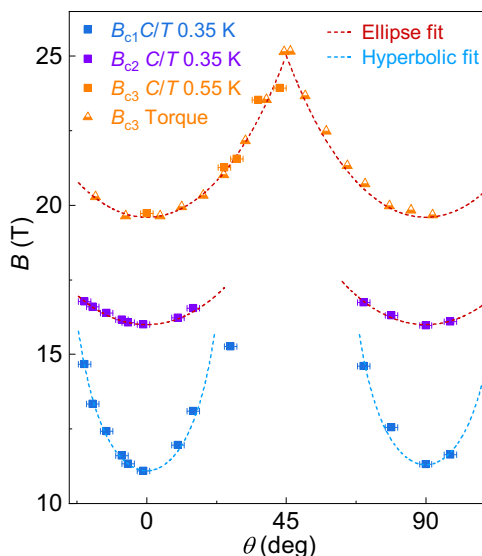
Fig. 3 | Angular dependence of double-peak structures. Angular dependence of B_{c1}, B_{c2}, and B_{c3} (square symbols). The magnetic field was applied from equivalent crystal axes [001] ($\theta = 0°$) to [010] ($\theta = 90°$) in the cubic structure of YbB$_{12}$. The angle dependence of B_{c3} marked as half-filled triangle symbols was extracted from the published magnetic torque data of Xiang et al.[2]. Red and blue dashed curves are the fits using ellipse and hyperbolic functions, respectively. The error bars are estimated from the misalignment between the sample and the Hall probe.

at fields of B' and B'' (Fig. 2b, c), which controls the double-peak structure of C/T. Since the splitting of the double peaks is $4.8k_BT$, the field dependence of $d\epsilon/dB$ is given by[28],

$$(B'' - B')\frac{d\epsilon}{dB} = 4.8k_BT \qquad (2)$$

Figure 2d shows the $(B'' - B')$ as a function of temperature for the four double-peak structures. From a linear fit, we estimate $d\epsilon/dB$ (from the inverse slope) for the four DoS singularities ($B_{c1}-B_{c4}$) to be 0.142 (0.025), 0.158 (0.015), 0.258 (0.015), 0.117 (0.01) meV/T, respectively.

Our observation of a double-peak structure in C/T that disperses linearly with increasing temperature is strong evidence for the existence of fermionic quasiparticles in the bulk[28], which is remarkable given the absence of an electronic DoS in the insulating bulk of YbB$_{12}$. It is equally important to note that the measured $1/T(B)$ from MCE, which is sensitive to the DoS at the Fermi energy[28], also induces a single-peak structure (Fig. 1c) in the same field regimes. Fitting to the double-peak structure in C/T at 19.6 T using Eq. (1) (Fig. S12, Supplementary Note 9) directly supports the origin of the fermionic DoS from a cusp-like singularity. The symmetric double-peak structure in C/T is a smoking gun signature for a symmetric cusp-like singularity in the DoS crossing the fermi energy. It is known that two-level crossing can show a similar double-peak structure in C/T, which is well characterized by the Schottky model[31–34]. However, this scenario is ruled out by the amplitude, magnetic field position, and number of levels of observed double-peak features in C/T (Supplementary Note 13). Alternative scenarios like the appearance of magnetic order and in-gap magnetic excitations are also considered and are found to be insufficient to account for these experimental observations (Supplementary Note 13).

Although both MCE and specific heat are bulk-sensitive probes, one may argue that the observed anomalies can be attributed to two-dimensional surface metallic states in YbB$_{12}$. However, it is important to note that the anomalies are "large", as they constitute a significant fraction of the total measured thermodynamic response. This already suggests that it has to be a bulk response, given that the total number of degrees of freedom on the surface is many orders of magnitude fewer

than in the bulk. Additionally, we performed a field sweep for C/T at different angles (Supplementary Note 7). The magnetic field is rotated from equivalent crystal axes [001] to [010] in a cubic structure. We extracted the field position ($B_{c1}-B_{c3}$) at which the DoS singularity meets the Fermi energy and plotted them as a function of angle θ in Fig. 3. θ is defined as the angle between B and [001]. The values for B_{c1}, B_{c2} and B_{c3} (marked as rectangular symbols) are extracted from the double-peak structure in C/T, while values for B_{c3} (marked as triangular symbols) are extracted from published magnetic torque data[2]. Interestingly, the three anomalies exhibit distinct angle dependencies. The singularity at B_{c1} follows a hyperbolic function, while the singularities at B_{c2} and B_{c3} can be fitted by the ellipse function with the same fitting parameters (Supplementary Note 7). All three anomalies exhibit a fourfold rotational symmetry, ruling out the possible 2D surface states. We therefore conclude that the DoS singularities at $B_{c1}-B_{c3}$ result from 3D bulk insulating states.

Discussion

The thermodynamic and transport experimental results indicate the existence of a series of in-gap discrete fermionic DoS singularities that are possibly consisting of charge-neutral quasi-particles. Driven by the magnetic field, this sequence of DoS singularities passes through the Fermi energy, which is reminiscent of Landau quantization. However, it is still premature to ascribe these oscillatory features to the quantum oscillations due to the limited number of DoS singularities and complex angular dependence.

Aside from quantum oscillation, the Lifshitz transition is also reported to show a double-peak structure in C/T, as demonstrated in the prototypical Kondo metal CeRu$_2$Si$_2$[28,35] and ferromagnetic superconductor UCoGe[28]. The origin of the Lifshitz transition in CeRu$_2$Si$_2$ was interpreted as a spin-split band passing over the fermi level with a DoS singularity pinned to the band edge[36,37]. This picture is consistent with our DoS singularities interpretation. Moreover, the DoS singularities in YbB$_{12}$ are cusp-like (Supplementary Note 9), which is often observed in Lifshitz transition[28]. However, it is commonly acknowledged that Lifshitz transitions yield kinks in Hall resistivity[37–40]. Except for the feature at 30 T, no corresponding anomaly was found in the Hall resistivity of YbB$_{12}$.

Although the formation mechanism of these DoS singularities remains elusive, it is worth comparing the experimental results with the available theoretical works to understand the unusual quasi-particles that constitute these singularities. Currently, the two main theoretical frameworks that have attempted to explain the magnetic-field-induced anomalous behavior in mixed-valence insulators have focused either on narrow-gap bulk insulators where the thermodynamic response involves thermally-activated gapped electrons[8–11,13,14,16] (Supplementary Note 11), or that involve a strong interaction-induced fractionalization of the electron, leading to the emergence of electrically neutral fermionic excitations (Supplementary Note 10)[6,7,12].

As noted above, it has been suggested that a variety of narrow-gap insulators can exhibit quantum oscillations and related phenomena[8–11,13,14,16], in the absence of any exotic fractionalized degrees of freedom contributing to the DoS at the Fermi energy. However, the finite gap associated with such insulators necessarily alters the temperature dependence of the overall amplitude associated with both the specific heat and MCE (Supplementary Note 11). For the temperature range of our measurement and based on the extracted charge gap scales from transport, such a clear exponential suppression of the measured thermodynamic quantities should have been self-evident. However, we do not observe any such activated behavior. Moreover, as shown in our calculation (Supplementary Note 11), the C/T in such a narrow-gap insulator does not show a double-peak feature in the absence of the gap closure.

In frustrated Mott-insulators with a small charge gap, it has been pointed out that electrically neutral spinon excitations can experience an effective orbital coupling to a magnetic field[41], resulting in quantum

oscillations in an insulator. Such oscillations have also been argued to be possible for small-gap mixed-valence insulators with Fermi surfaces of emergent neutral fermions[6,7,12] (Supplementary Note 10). The double-peak features in C/T are demonstrated to be observed in this scenario (Supplementary Note 10). Therefore, the quasiparticles that account for our observation are possibly related to interaction-induced electron-fractionalization.

We have observed, in the insulating phase of YbB$_{12}$, a series of fermionic DoS singularities passing through the Fermi energy at 11, 16, 19.6, and 30 T, respectively. Except for the feature at 30 T, no corresponding anomaly was found in the Hall resistivity, ruling out the relevance of itinerant electrons for the observations. The relatively large magnitude of the effect, its angular dependence, and its field and temperature-dependence, reveals a highly unusual physical phenomenon, where a three-dimensional insulating bulk behaves like a conventional metal in the absence of electrically conducting electrons. Future theoretical research will need to address a microscopic theory for the origin of such unusual phenomena in the regime of strong correlations, and will benefit from complementary spectroscopic experiments that directly probe multiparticle correlations associated with the low-energy fractionalized degrees of freedom.

Methods

Sample preparation
The YbB$_{12}$ single-crystal samples were grown by the floating zone method. The samples were cut from the ingots and polished into a rectangular shape. The sample plane corresponds to the (100) surface of the crystal. The dimension and weight are ~1.1 × 0.9 × 0.05 mm^3 and ~0.3 mg for Sample#1, ~1 × 1 × 0.5 mm^3 and ~2.3 mg for Sample#2, ~0.5 × 0.5 × 0.16 mm^3 and ~0.2 mg for Sample#3, and ~1.1 × 0.6 × 0.05 mm^3 and ~0.2 mg for Sample #4.

Magneto-transport and magneto-caloric effect measurement in pulsed magnetic field
Magnetocaloric effect and part of the magneto-transport measurements were performed using a non-destructive pulse magnet at the International Megagauss Laboratory at ISSP, the University of Tokyo. The maximal field and pulse duration of the magnet are about 60 T and 36 ms, respectively.

For transport measurements, the longitudinal magnetoresistance ρ_{xx} and Hall resistivity ρ_{xy} were measured simultaneously on the same sample using the standard 6 probe method. Thirty micrometre gold wires were attached to the sample by the silver paint, resulting in a contact resistance of less than 10 Ω. During the measurement, a 600 μA AC current with a frequency of 80 kHz was applied to the sample. A homemade ^{3}He system was used to cool the sample down to 0.6 K.

For MCE measurements, a 500 nm SU-8 2000.5 epoxy-based photoresist was prepared on the surface of the sample as the insulating layer. A Au$_{16}$Ge$_{84}$ thin film thermometer was then sputtered on the insulating layer and calibrated to the reference thermometer. The temperature of the sample was monitored and recorded during the pulse field sweeps. For both measurements, the magnetic field was applied along [1 0 0] direction.

Magneto-transport measurement in a static magnetic field
Part of the magneto-transport measurements were performed under a static magnetic field condition in the Institute for Material Research (IMR), Tohoku University. The maximal field of the superconducting magnet in IMR is about 25 T.

For the transport measurement in static magnetic field, the sample preparation was the same as in the pulsed magnetic field case. Due to the slow field sweep rate in static magnetic field, a lower AC current (30 μA) with a lower frequency (10 Hz) was applied to the sample. The homemade ^{3}He system in IMR was able to cool down the sample down to 0.52 K.

Specific heat measurement in a static magnetic field
AC-specific heat measurements were carried out in a static magnetic field at the Laboratoire National des Champs Magnétiques Intenses–Grenoble. The maximal field of the resistive magnet in LNCMI-G is about 35 T.

During the experiment, the specimen was attached to the back-side of a bare CERNOX resistive chip by a minute amount of Apiezon grease. The resistive chip was split into heater and thermometer parts by artificially making a notch along the middle line of the chip. The heater part was used to generate a periodically modulated heating power P_{ac} with a frequency of 2ω, which can be described as the following relation,

$$P_{ac} = \frac{R_H i_{ac}^2}{2\omega} \tag{3}$$

where R_H is the resistance of the heater part, i_{ac} is a modulating current with a frequency of ω. The induced oscillating temperature T_{ac} of the sample was monitored by the thermometer part of the resistive chip. To do so, we applied a reading current i_T at an odd harmonic $n\omega$ and monitored the induced AC voltage V_{ac} at $(n+2)\omega$. Based on a precise calibration of the thermometer (R–T relation), T_{ac} can be calculated from,

$$V_{ac}([n+2]\omega) = \frac{dR_T}{2dT} T_{ac}(2\omega) i_T([n+2]\omega) \tag{4}$$

Knowing P_{ac} and T_{ac}, specific heat can be calculated by[42]

$$C = \frac{P_{ac}|\sin(\phi)|}{2\omega|T_{ac}|} \tag{5}$$

Here, φ stands for the phase shift between P$_{ac}$ and T$_{ac}$. To optimize the signal over noise ratio, the measurement frequency (ω) is chosen to keep the phase shift in the range −90° < φ < −30°.

The angle dependence of the specific heat was measured by a Hall probe equipped with an Attocube rotator. During the measurement, the CERNOX resistor was mounted on a copper ring attached to an Attocube rotator. The back of the copper ring was attached to the Hall probe, which allows to measure the angle under the magnetic field. The misalignment between the sample and the Hall probe is estimated to be within ± 2°.

Data availability
Source data are provided in this paper. All other data that support the findings of this study are available upon request to the corresponding author. Source data are provided in this paper.

References
1. Tan, B. et al. Unconventional Fermi surface in an insulating state. *Science* **349**, 287–290 (2015).
2. Xiang, Z. et al. Quantum oscillations of electrical resistivity in an insulator. *Science* **362**, 65–69 (2018).
3. Li, G. et al. Two-dimensional Fermi surfaces in Kondo insulator SmB$_6$. *Science* **346**, 1208–1212 (2014).
4. Wang, P. et al. Review of Scientific InstrumentsLandau quantization and highly mobile fermions in an insulator. *Nature* **589**, 225–229 (2021).
5. Xiao, D., Liu, C.-X., Samarth, N. & Hu, L.-H. Anomalous quantum oscillations of interacting electron-hole gases in inverted type-II InAs/GaSb quantum wells. *Phys. Rev. Lett.* **122**, 186802 (2019).
6. Chowdhury, D., Sodemann, I. & Senthil, T. Mixed-valence insulators with neutral Fermi surfaces. *Nat. Commun.* **9**, 1766 (2018).
7. Sodemann, I., Chowdhury, D. & Senthil, T. Quantum oscillations in insulators with neutral Fermi surfaces. *Phys. Rev. B* **97**, 045152 (2018).

8. Knolle, J. & Cooper, N. R. Quantum oscillations without a Fermi surface and the anomalous de Haas-van Alphen effect. *Phys. Rev. Lett.* **115**, 146401 (2015).

9. Knolle, J. & Cooper, N. R. Excitons in topological Kondo insulators: theory of thermodynamic and transport anomalies in SmB_6. *Phys. Rev. Lett.* **118**, 096604 (2017).

10. Zhang, L., Song, X.-Y. & Wang, F. Quantum oscillation in narrow-gap topological insulators. *Phys. Rev. Lett.* **116**, 046404 (2016).

11. Shen, H. & Fu, L. Quantum oscillation from in-gap states and a Non-Hermitian Landau level problem. *Phys. Rev. Lett.* **121**, 026403 (2018).

12. Erten, O., Ghaemi, P. & Coleman, P. Kondo breakdown and quantum oscillations in SmB_6. *Phys. Rev. Lett.* **116**, 046403 (2016).

13. Ram, P. & Kumar, B. Theory of quantum oscillations of magnetization in Kondo insulators. *Phys. Rev. B* **96**, 075115 (2017).

14. Knolle, J. & Cooper, N. R. Anomalous de Haas-van Alphen effect in InAs/GaSb quantum wells. *Phys. Rev. Lett.* **118**, 176801 (2017).

15. Varma, C. Majoranas in mixed-valence insulators. *Phys. Rev. B* **102**, 155145 (2020).

16. Panda, A., Banerjee, S. & Randeria, M. Quantum oscillations in the magnetization and density of states of insulators. *Proc. Natl. Acad. Sci. USA.* **119**, e2208373119 (2022).

17. Sato, Y. et al. Unconventional thermal metallic state of charge-neutral fermions in an insulator. *Nat. Phys.* **15**, 954–959 (2019).

18. Xiang, Z. et al. Hall anomaly, quantum oscillations and possible Lifshitz transitions in Kondo insulator YbB_{12}: evidence for unconventional charge transport. *Phys. Rev. X* **12**, 021050 (2022).

19. Adams, E. N. & Holstein, T. D. Quantum theory of transverse galvano-magnetic phenomena. *J. Phys. Chem. Solids* **10**, 254–276 (1959).

20. Lifshitz, I. & Kosevich, A. Theory of magnetic susceptibility in metals at low temperatures. *Sov. Phys. JETP* **2**, 636–645 (1956).

21. Kawasaki, S. et al. Temperature dependence of metamagnetic transition in YbB_{12}. *Physica B* **281**, 269–270 (2000).

22. Mizzi, C. A. et al. The reverse quantum limit: implications for unconventional quantum oscillations in YbB_{12}. *Nat. Commun.* **15**, 1607 (2024).

23. Sugiyama, K., Iga, F., Kasaya, M., Kasuya, T. & Date, M. Field-induced metallic state in YbB_{12} under high magnetic field. *J. Phys. Soc. Jpn* **57**, 3946–3953 (1988).

24. Terashima, T. T. et al. Magnetization process of the Kondo insulator YbB_{12} in ultrahigh magnetic fields. *J. Phys. Soc. Jpn* **86**, 054710 (2017).

25. Liu, H. et al. Fermi surfaces in Kondo insulators. *J. Condens. Matter Phys.* **30**, 16LT01 (2018).

26. Thomas, S. M. et al. Quantum oscillations in flux-grown SmB_6 with embedded aluminum. *Phys. Rev. Lett.* **122**, 166401 (2019).

27. Okawa, M. et al. Hybridization gap formation in the Kondo insulator YbB_{12} observed using time-resolved photoemission spectroscopy. *Phys. Rev. B* **92**, 161108 (2015).

28. Yang, Z. et al. Unveiling the double-peak structure of quantum oscillations in the specific heat. *Nat. Commun.* **14**, 7006 (2023).

29. Woollam, J. A. Graphite carrier locations and quantum transport to 10 T (100 kG). *Phys. Rev. B* **3**, 1148 (1971).

30. Kittel, C. & McEuen, P. *Kittel's Introduction to Solid State Physics.* (John Wiley & Sons, 2018).

31. Richter, J., Krupnitska, O., Baliha, V., Krokhmalskii, T. & Derzhko, O. Thermodynamic properties of $Ba_2CoSi_2O_6Cl_2$ in a strong magnetic field: Realization of flat-band physics in a highly frustrated quantum magnet. *Phys. Rev. B* **97**, 024405 (2018).

32. Affronte, M. et al. Mixing of magnetic states in a Cr_8 molecular ring. *Phys. Rev. B* **68**, 104403 (2003).

33. Rosenfeld, E. V. Crossover and splitting of the heat capacity peak. *Solid State Commun.* **153**, 23–25 (2013).

34. Gopal, E. *Specific Heats at Low Temperatures.* (Springer Science & Business Media, 2012).

35. Aoki, Y. et al. Thermal properties of metamagnetic transition in heavy-fermion systems. *J. Magn. Magn. Mater.* **177-181**, 271–276 (1998).

36. Pfau, H., Daou, R., Brando, M. & Steglich, F. Thermoelectric transport across the metamagnetic transition of $CeRu_2Si_2$. *Phys. Rev. B* **85**, 035127 (2012).

37. Daou, R., Bergemann, C. & Julian, S. R. Continuous evolution of the Fermi surface of $CeRu_2Si_2$ across the metamagnetic transition. *Phys. Rev. Lett.* **96**, 026401 (2006).

38. Pfau, H. et al. Interplay between Kondo suppression and Lifshitz transitions in $YbRh_2Si_2$ at high magnetic fields. *Phys. Rev. Lett.* **110**, 256403 (2013).

39. Pfau, H. et al. Cascade of magnetic-field-induced Lifshitz transitions in the ferromagnetic Kondo lattice material $YbNi_4P_2$. *Phys. Rev. Lett.* **119**, 126402 (2017).

40. Pourret, A. et al. Transport spectroscopy of the field induced cascade of Lifshitz transitions in $YbRh_2Si_2$. *J. Phys. Soc. Japan* **88**, 104702 (2019).

41. Motrunich, O. I. Orbital magnetic field effects in spin liquid with spinon Fermi sea: Possible application to $k\text{-}(ET)_2Cu_2(CN)_3$. *Phys. Rev. B* **73**, 155115 (2006).

42. Kohama, Y., Marcenat, C., Klein, T. & Jaime, M. AC measurement of heat capacity and magnetocaloric effect for pulsed magnetic fields. *Rev. Sci. Instrum.* **81**, 104902 (2010).

Acknowledgements

Author contributions

Z.Y. and Y.K. conceived the study. F.I. grew the high-quality YbB_{12} sample. Z.Y., M.K., and Y.K. conducted the magnetotransport experiments. Z.Y., S.I., and Y.K. conducted the magnetocaloric effect experiment. C.M., A.M., and T.K. conducted the specific heat experiments. Z.Y., T.N., D.K.M., and Y.K. analyzed the experimental data. S.K. and D.C. provided theoretical support. Z.Y., Y.K., C.M., T.K., S.K., and D.C. prepared the paper, with input from all other co-authors.

Competing interests

The authors declare no competing interests.

Additional information

Supplementary information The online version contains supplementary material available at https://doi.org/10.1038/s41467-024-52017-x.

Correspondence and requests for materials should be addressed to Christophe Marcenat, Debanjan Chowdhury or Yoshimitsu Kohama.

Peer review information *Nature Communications* thanks Neil Harrison and the other, anonymous, reviewer for their contribution to the peer review of this work. A peer review file is available.

Reprints and permissions information is available at http://www.nature.com/reprints

Publisher's note Springer Nature remains neutral with regard to jurisdictional claims in published maps and institutional affiliations.